STRUCTURAL INVESTIGATION OF SiC_f/SiC COMPOSITES

H. Tatlisu, M. Bastuerk, H. Rauch, M. Trinker

Atomic Institute of the Austrian Universities, Stadionallee 2 A-1020, Vienna, Austria
tatlisu@ati.ac.at

Keywords:

SiC composites, neutron imaging, small angle neutron scatering

Abstract

Ceramic matrix composites (CMC), especially silicon carbide (SiC) fiber-reinforced silicon carbide (SiC) matrix composites (SiC_f/SiC) developed for high temperature applications are currently under discussion as a first wall and structural material for future fusion power plants. Porosity and radiation-induced swelling in the CMC and their influence on the thermal conductivity are the major problems. In addition, they affect the onset of the radiation damage parameters in a high radiation environment.

The objective of this paper is to analyze the structure of the SiC_f/SiC composite and to understand the radiation effects induced by neutrons and protons in a SiC_f/SiC composite. In order to investigate radiation-induced structural changes on a micro- and nanostructural scale, a SiC_f/SiC composite has been exposed to high proton and neutron radiation in the SINQ spallation source. To analyze of the structural changes, e.g. pore sizes, a highly irradiated and a non-irradiated SiC_f/SiC composite have been inspected by means of small angle neutron scattering at the Paul Scherrer Institute (PSI). Non-irradiated SiC_f/SiC composites have been investigated with neutron radiography and scanning electron microscopy. These different methods for material investigations give an insight into the properties of this material in view of its applications in future fusion power plant.

1. Introduction

The SiC_f/SiC composite is being considered as a candidate material in the first wall design and blankets of a future fusion reactor because of its outstanding high thermal conductivity, high-temperature strength retention up to 1200 C and exceptional radiation stability in a high radiation environment [1]. The thermal conductivity is an important factor for the first wall material, because main function of the first wall is to remove the power generated by the high energetic neutrons and alpha particles resulting from fusion within the plasma.

N3-1 SiC_f/SiC composites manufactured by SNECMA using a chemical vapour infiltration (CVI) method, have a 3-dimensional texture which consists of Nicalon Si-C-O fibers (Nippon Carbon Co., Ltd) in a SiC matrix [2]. CVI is an effective but slow process for manufacturing ceramic matrix composites. Unfortunately, some unavoidable residual porosity is created during the CVI process. Porosity, introduced during manufacturing of the composites, causes degradation in the thermal conductivity and radiation stability of SiC_f/SiC composites. Pore sizes can vary over a wide range from micropores (< 2 nm) and mesopores (2-50 nm) to macropores (> 50 nm). The porosity has to be controlled if usable composites are to be produced.

First wall and blanket structure materials in a future fusion reactor will be exposed to a high energy neutron flux up to 14 MeV. The SiC_f/SiC composites in a radiation environment have to retain their properties during the lifetime of a fusion reactor. Therefore, a 2 mm thick N3-1 SiC_f/SiC composite has been irradiated to fluencies of $\sim 5.8 \times 10^{25}$ neutrons/m^2 and $\sim 2.5 \times 10^{25}$ protons/m^2 in the SINQ target for 16 months to study the radiation-induced porosity and structural changes in the SiC_f/SiC composite. The neutron and proton spectra have been calculated with the MCNPX code. The temperature of the composite during the irradiation time was calculated to be around 200 °C.

2. Experimental

2.1 Inspection by SEM and Neutron Imaging Techniques

Imaging techniques are necessary to visualize the structure, structural changes, and possible defects in SiC_f/SiC composites. Scanning electron microscopy (SEM) is routinely used for the characterization of the SiC_f/SiC composites and is a reliable and fast method to obtain images of the surface structure. The SiC_f/SiC composites investigated by the SEM method possess inherent pores with different sizes, which can be seen in Fig. 1b. The large pores, so-called macropores, are visible between fiber bundles, while much smaller pores could not be seen very clearly. The fibers (diameter around 14 μm) are inserted into the SiC matrix as shown in Fig. 1a. The fiber bundles consist of different sizes of SiC fibers, as seen in Fig. 1b.

In order to reveal the inner structure of the SiC_f/SiC composite, different neutron imaging methods have been used. Neutron radiography (NR) is a very challenging imaging technique in the investigation of light elements like H, D, B and Li, and its isotope sensitivity makes it very attractive to obtain better contrast between neighbouring elements in the periodic chart [3]. Therefore, the SiC_f/SiC composites were investigated by different neutron imaging methods. The neutron attenuation coefficients of elements depend strongly on the neutron energy, and consequently on the neutron spectrum. Thermal neutron radiography using a thermal neutron spectrum gives very good contrast for the investigation of most samples. Some samples, however, like the SiC_f/SiC composite with low neutron attenuation could not be visualized by means of thermal NR. A 3 mm thick non-irradiated SiC_f/SiC composite was investigated by thermal NR as seen in Fig. 2a. As a detection system, a neutron sensitive scintillator based CCD camera was

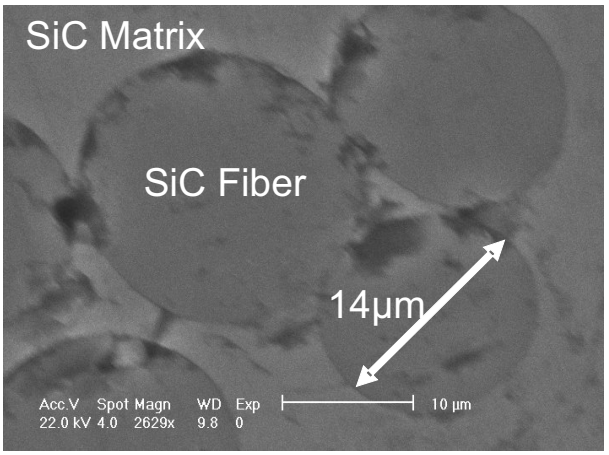

a)

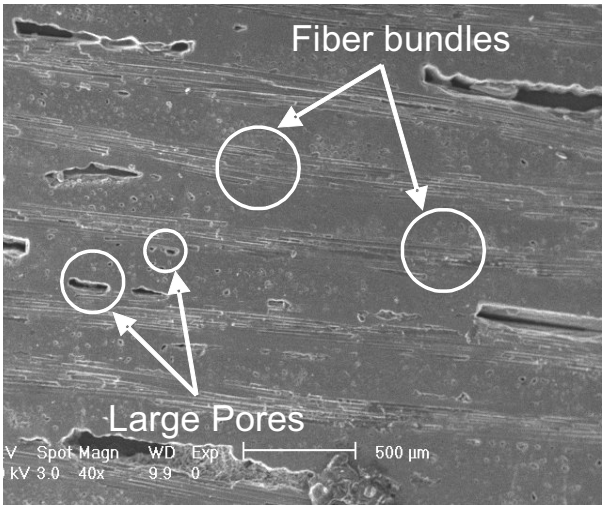

b)

Figure 1. SEM micrographs showing (a) Nicalon SiC fibers with a diameter of about 14 µm. (b) Surface area with different size pores and fibers bundles.

used. As seen on the images, SiC_f/SiC composite has very low neutron attenuation characteristics and very low image contrast could be obtained. In order to increase contrast or neutron attenuation, two non-irradiated SiC_f/SiC composites together, each having 3 mm of thickness, were inspected. The thermal NR shows a homogenous SiC/SiC structure. Thereafter, energy selective neutron radiography (ESNR), using monochromatic neutrons with a broad spectrum, was applied to the composites at the PGA-PSI in Switzerland [4]. Unfortunately, the facility PGA doesn't exist anymore at the PSI, it was replaced by another experimental setup. The spectrum gets broader at poor energy resolution (30 % at 10 Å). Monochromatization was done using a velocity selector and a digital detection system based on scintillator/CCD camera was used. Fig. 2b shows ESNR images from the same composite recorded at 2.6 Å and 7.9 Å respectively. The neutron attenuation coefficients of Si and C elements are different at different neutron spectra; therefore the ESNR method delivered better image contrast between fiber bundles and pores, more structural details showing the woven structure of SiC/SiC fiber bundles. Recently, neutron imaging with coherent thermal neutrons has been exploited to investigate very low contrast objects, so-called phase objects [5, 6]. In this

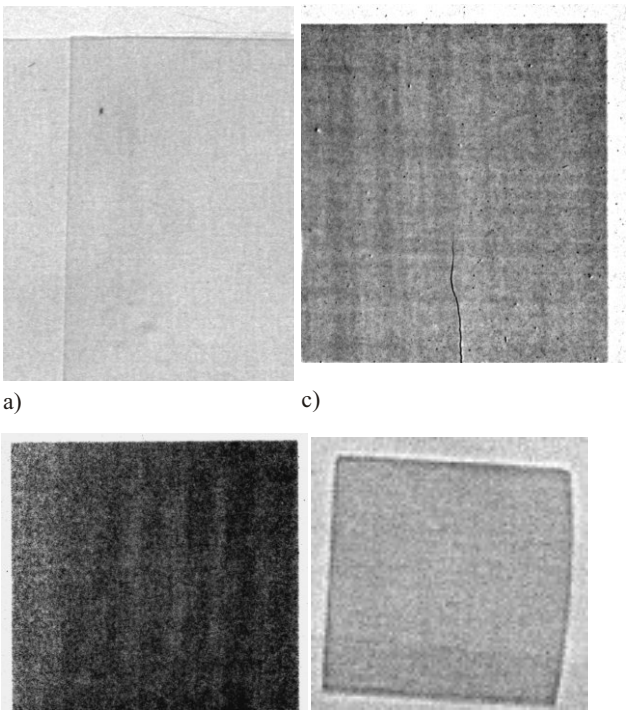

a) c)

b) d)

Figure 2. NR images of the non-irradiated SiC_f/SiC composites taken by: a) thermal NR with 0.5 mm resolution, b) ESNR at 2.6 Å with ~ 0.4 mm spatial resolution, c) ESNR at 7.9 Å with ~ 0.9 mm spatial resolution and d) phase contrast NR with 0.1 mm resolution.

method, a 1 mm small hole in a thin Gd foil is used to vary neutron collimation with a combination of different pinhole-sample and sample-detector distances. The drawback of this method is that it needs longer exposure time (2 hours) due to the lower neutron intensity. On the other hand, high resolution neutron sensitive IPs (Imaging Plates) with 100 micrometer spatial resolution were used as a detection screen at the PSI in Switzerland. The image contrast at the edges was increased; however, no structural information could be obtained. The refraction-related bright and dark fringes caused a contrast increase at the edges as seen in Fig. 2c.

As seen in Fig. 2, the contrast depends strongly on the Bragg-cutoff energy as a function of used beam spectrum in ESNR images. More structural information could be obtained from ESNR images in spite of higher spatial resolution. The images obtained by ESNR shows clearly the fiber bundles and porosity. The fibers and matrix both consist of homogenous SiC material having the same neutron attenuation coefficients, and therefore the contrast seen on the images should be an indicator of the existence of pores.

2.2. Small Angle Neutron Scattering (SANS)

SANS measurements were carried out at the SANS-I facility of the PSI-Switzerland [7]. This instrument covers a Q-range of 6 10^{-3} nm^{-1} < Q < 10.5 nm^{-1}. The scattering patterns for both irradiated and non-irradiated composites were recorded at four different instrumental configurations with the samples perpendicular to the incoming neutron beam, corresponding to the orientation in Fig. 2: sam-

ple-detector distances of 2.0, 6.0, 20.0 m with neutron wavelength = 4.7 Å, and a sample-detector distance of 20.0 m with neutron wavelength = 18 Å. For both composites, the scattering patterns exhibit a partially anisotropic behaviour and symmetry around the horizontal and vertical axis as seen in the inset of Fig. 3. These two axes correspond to the main orientation of the woven fibers in the composite [2]. The pores show elongation along the fibres. This oriented nature of the pore structure in SiC_f/SiC composites was also observed in a previous study [8]. These composites can be treated as a two-phase system consisting of pores and matrix with constant scattering length densities. The scattering length density difference between fibers, matrix and on the components of the SiC_f/SiC composites has been calculated as = 4.784×10^{10} cm^{-2}. For the evaluation of scattering data from porous media the Debye-Anderson-Brumberger (DAB) model can be applied [9]. In our modification of the model two different pore types with correlation length l_0 and l_1 are assumed [6]. To account for the anisotropic nature of the scattering patterns the data are averaged over narrow segments (width 10°) and the modified DAB-model Eq.1 is fitted to the experimental data

$$\frac{d}{d}(Q) \quad 8 \left(\quad \right)^2 \frac{\overline{l_0^3}_{\ 0}(1 \quad _0)}{(1 \quad Q^2 l_0^2)^2} \quad \frac{\overline{l_1^3}_{\ 1}(1 \quad _1)}{(1 \quad Q^2 l_1^2)^2} \quad bcg \quad (1)$$

where and are the volume fractions of the two pore types, and $\frac{d}{d}(Q)$ is the macroscopic differential scattering cross section usually given in absolute units (cm^{-1}), see Fig. 3. With this model correlation lengths and volume fractions of the porosity can be determined.

The two pore types were classified as the small and the large pore type, see Figure 4. The average diameter for large pores of the non-irradiated and the irradiated composite was estimated to be around 1045 Å (volume fraction 0.27 ± 0.06%) and 709 Å (volume fraction 0.48 ± 0.06%), respectively. This shows that the average diameter for large pores was decreased by the irradiation. The average diameter for small pores in the non-irradiated and irradiated composites were calculated as 4.8 Å (volume fraction 6.740 ± 1.24%) and 32.0 Å (volume fraction 0.11 ± 0.04%), respectively. The average diameter for small pores was increased by irradiation, its volume fraction, however, decreased considerably.

3. Conclusion and outlook

In order to determine the most efficient imaging experiments, the non-irradiated SiC/SiC composite was investigated with different NR methods: thermal NR, ESNR and phase contrast NR. Among these methods, ESNR delivered the best image contrast. Phase contrast NR is very promising in the investigation of low contrast materials, however improvement in its detection system is necessary.

Radiation stability data of the SiC_f/SiC composites are still inadequate, and more irradiated composites are certainly required to understand the radiation caused structural changes in the SiC_f/SiC composite. Pores larger than our calculated pore dimensions also exist in the SiC_f/SiC

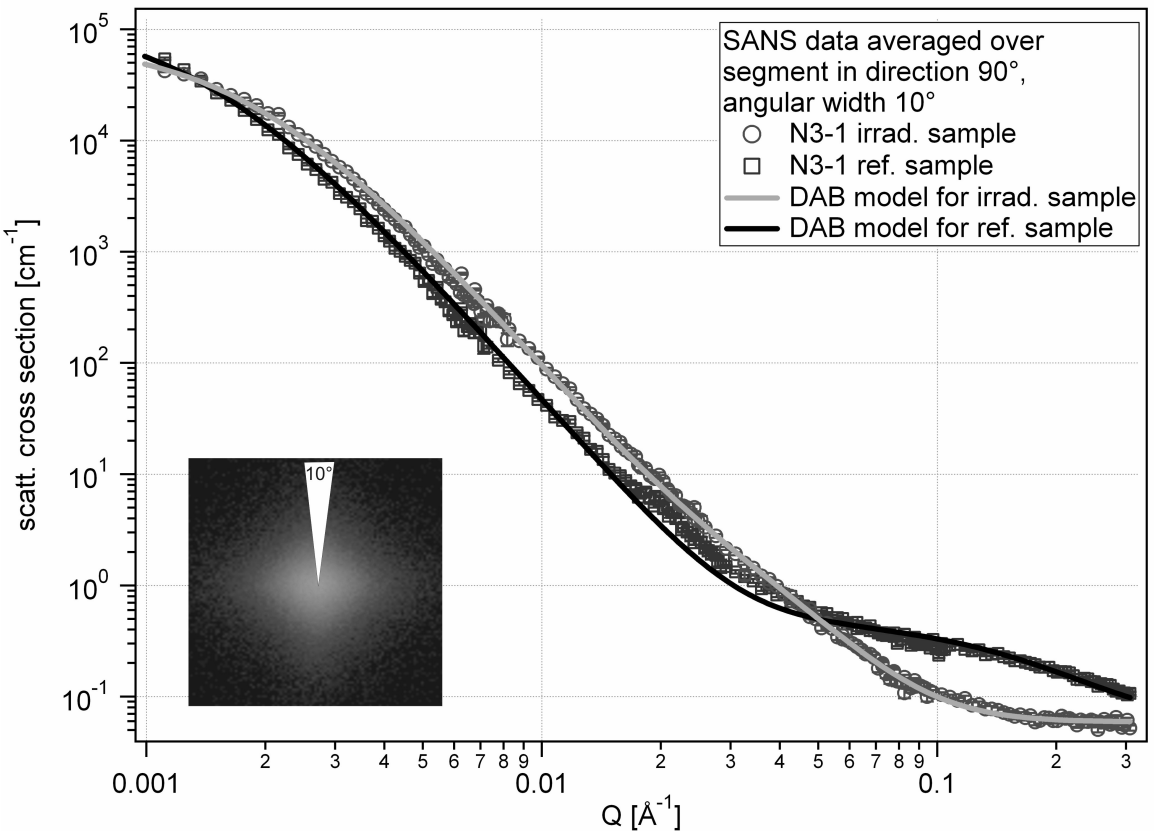

Figure 3. Scattering cross section averaged over a sector (angular width 10°) for both irradiated and non-irradiated sample [4].

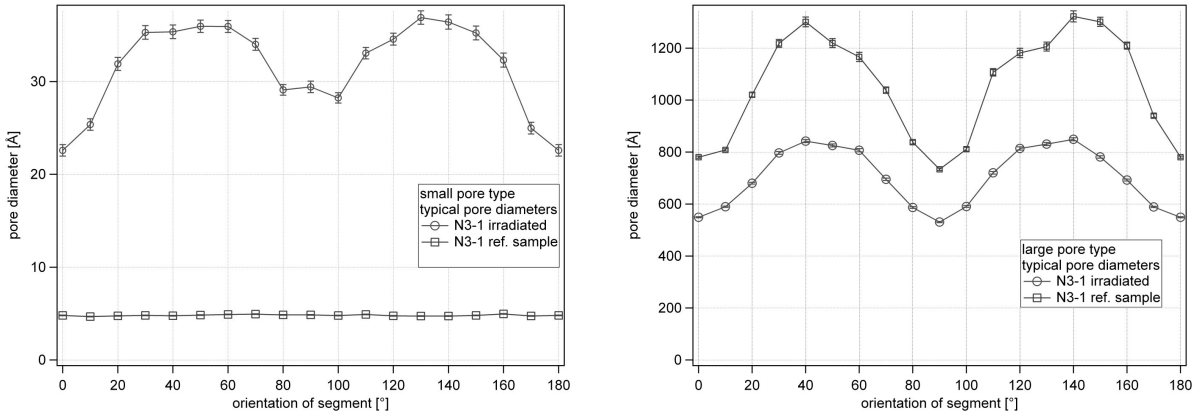

Figure 4. The fit parameters (left) and (right) for the irradiated and the reference sample for different orientations of the segment over which scattering data were averaged. These length parameters can be interpreted as average pore diameters.

composite, which could not be observed in SANS measurements due to the limited Q-range. Therefore, ultra small angle neutron scattering (USANS) technique will be carried out to determine the large pores.

In order to improve the composite structure and radiation stability, the newly developed Tyranno SA and Hi-Nicalon Type-S fibers based composites have to be investigated for a definitive understanding of structure changes in composites.

Acknowledgments

We would like to thank J. Kohlbrecher and G. Kühne for their technical support during the measurements at the PSI-Switzerland and M. Austerer for his helps during the SEM measurement at the Institute for Solid State Electronics at the Vienna University of Technology.

This work has been carried out within the Association EURATOM-ÖAW.

References

1. Y. Katoh, L.L. Snead, T. Nozawa, N.B. Morley, W.E. Windes, *Adv. in Sci. and Tech.* **45** (2006) 1915-1924.
2. B. Riccardi, L. Giancarli, A. Hasegawa, Y. Katoh, A. Kohyama, R. H. Jones, L.L. Snead, *J. Nucl. Materials*, **329-333** (2004) 56-65.
3. M. Bastürk, J. Arztmann, W. Jerlich, N. Kardjilov, E. Lehmann and M. Zawisky, *J. Nucl. Materials*, **341** (2005), 189-200.
4. N. Kardjilov, S. Baechler, M. Bastürk, M. Dierick, J. Jolie, E. Lehmann, T. Materna, B. Schillinger and P. Vontobel, *Nucl. Instr. Meth. A* **501** (2003), 536-546.
5. M. Bastürk, N. Kardjilov, H. Rauch, P. Vontobel, *Nucl. Inst. Meth. A*, **542** (2005), 106-115.
6. M. Bastuerk, Y. Dai, H. Rauch, and M. Trinker, *Nucl. Instr. Meth. A* **564** (2006) 431-438.
7. J. Kohlbrecher and W. Wagner, *J. Appl. Cryst*. **33** (2000) 804.
8. M. Hainbuchner, M. Villa, M. Baron, J. Kohlbrecher, H. Rauch, Conference Proceedings of the 4th IEA Workshop, Frascati, Italy, October, (2001), 12-13.
9. P. Debye, H.R. Anderson, H. Brumberger, *J. Appl. Phys.* **28** (1957) 679.